NASA TECHNICAL NOTE

NASA TN D-2405

LOAN COPY: RE
AFWL (WL
KIRTLAND AFB

TECH LIBRARY KAFB, NM
0154896

NASA TN D-2405

RADIOMETER-PYROMETER FOR ANALYSIS OF GASEOUS COMBUSTION PRODUCTS

by Donald R. Buchele

Lewis Research Center

Cleveland, Ohio

NATIONAL AERONAUTICS AND SPACE ADMINISTRATION • WASHINGTON, D. C. • AUGUST 1964

TECH LIBRARY KAFB, NM
0154896

RADIOMETER-PYROMETER FOR ANALYSIS OF GASEOUS COMBUSTION PRODUCTS

By Donald R. Buchele

Lewis Research Center
Cleveland, Ohio

NATIONAL AERONAUTICS AND SPACE ADMINISTRATION

For sale by the Office of Technical Services, Department of Commerce,
Washington, D.C. 20230 -- Price $0.50

RADIOMETER-PYROMETER FOR ANALYSIS OF GASEOUS COMBUSTION PRODUCTS

by Donald R. Buchele

Lewis Research Center

SUMMARY

A radiometer-pyrometer was developed for the measurement of absorption, emission, and temperature of gases. Spectral selection was by filters over a wavelength range limited by fused-quartz optics with a choice of three detectors. Radiation of an external source and an internal source was intercompared by chopping at 120 cycles per second. Absolute radiation from the hydroxyl group (OH) and water (H_2O) in the combustion products of natural gas and gasoline was measured.

INTRODUCTION

The instrument described in this paper was initially designed for studying recombination of the hydroxyl group (OH) and hydrogen (H) in the gaseous products of hydrogen-air combustion as they expand through a nozzle. It was believed that the partial pressure of OH could be estimated from the ratio of the total radiation from the OH band centered at 3100 A (0.31 μ) to the total radiation from the water (H_2O) band centered at 1.9 microns. The instrument was thus designed to measure radiation from up to six bands. This capability also permitted deduction of the gas temperature by the absorption-emission method (refs. 1 to 5). Since bands are selected by use of readily changed filters, the instrument has wider utility than its initial application and could serve as radiometer, pyrometer, or gas analyzer for other high-temperature gas mixtures.

Principle

The instrument, similar to some others described in the literature, provides continuous sampling of two fluxes with one filter along the same optical path. The fluxes are sampled periodically by use of a light chopper that exposes the detector to four fluxes: external ("flame") radiation, radiation from an internal reference lamp, external radiation plus radiation from an external comparison lamp (if temperature is to be measured), and zero flux (darkness). Various combinations of sources, detectors, choppers, and beam splitters that may be chosen for such a sampling technique are considered in references 6 and 7.

Methods of Achieving Accuracy

Some limitations to measurement accuracy and methods of overcoming them are as follows:

(1) Nonuniform sensitivity. Experience has shown that the sensitivity of most radiation detectors varies with time, temperature, fatigue, and other factors so that the error of absolute flux measurements is generally greater than 1 percent (ref. 8). For example, reference 9 minimized the effect of nonuniform spectral sensitivity over the surface of a multiplier phototube with a ground-quartz diffusing window in front of the phototube. Nonuniform sensitivity has been studied in references 10 to 14. By providing an internal reference lamp that has greater long-term stability than the detector and alternately measuring the reference and the sample radiation with the same detector, accuracy approaching the reference can be obtained. This principle has long been used in optical pyrometers, and it is successfully applied to automatic pyrometers (refs. 15 to 18), radiometers (refs. 19 and 20), and other commercial instruments not reported in the literature.

(2) Nonlinearity. When the internal reference lamp is operated at a fixed temperature, a ratio of the sample radiation to the reference can be obtained. Large ratios, however, require a detector with linear response or a calibrated nonlinear detector. Also, large ratios may be subject to error in the smaller flux measurement caused by the addition of stray radiation from the larger flux. By attenuating the internal reference source with an aperture, an approximate match to the sample radiation within a 10:1 ratio can be made. The detector linearity requirement is thereby lessened, and the linearity errors are minimized. This method is used in the present instrument, with four beam attenuators giving a reference-lamp-flux range of 10^6. In addition, the reference-lamp current is continuously variable and gives an additional flux range of 10^2.

(3) Poor absolute accuracy. By using the internal reference lamp as a transfer device, the ratio of intensity of an external sample source to intensity of an external standard source becomes the actual measurement. Available external standard spectral sources are commercial blackbody cavities of 1000° C and a tungsten-ribbon lamp calibrated by the National Bureau of Standards as a spectral standard of radiation (ref. 21).

(4) Wide range of intensities. A limitation of the thermal radiator as an external standard source is the wide variation of intensity with wavelength in accordance with the Planck spectral distribution. In the ultraviolet, the intensity of a 2860° K blackbody changes greatly for even a slight change of wavelength so that, for example, from a peak intensity at 1 micron it is reduced by a factor of 10^5 at 0.2 micron. Thus, over a wide range of wavelengths, an incandescent lamp is far from an ideal spectrally independent source. This fact tends to complicate its use as a reference by which a measurement is divided. The complication is minimized in applications such as automatic pyrometers, where the utilized wavelength range of the lamp is limited or fixed. It frequently happens that the radiation to be measured also approximates the Planck distribution, so that the ratio does not change

appreciably with wavelength. The wide range of intensity level is covered in this instrument with detector apertures giving an attenuation range of 10^3 and amplifier gain that is variable over a range of 10^3.

(5) Wide range of wavelengths. No one detector is best at all wavelengths. The detection improves as the range of detector response is confined to the short wavelengths, where a photon has greater energy and ambient radiation is small. Thus, the photoemissive detector limited to the ultraviolet and visible spectrum is superior to a photoconductor, which responds to the ultraviolet through the near infrared spectrum; this in turn is superior to the thermal detector, which responds to the far infrared as well. A choice of three detectors is provided in this instrument to obtain the best detection at any wavelength.

The major problems involved in spectroradiometric measurements have been discussed; the noteworthy techniques used to solve these problems will be described in the following section. The theory applicable to the design and the preliminary test results will then be given.

DESIGN AND OPERATION

Layout

The instrument structure is a metal box supported on rubber vibration mounts inside another metal box (fig. 1(a)). The inner box is divided into three light-tight compartments containing the detectors, the internal reference lamp, and the chopper, respectively. The optical paths of both the gas radiation transmitted through the focusing lens and the internal reference lamp radiation transmitted through the reference lamp condensing lens meet at the reflecting chopper. The radiation leaving the chopper is transmitted through the filter and aperture disks to the detector, which is mounted on a sliding platform. Any one of three detectors or a viewing telescope mounted on the platform can be selected. In addition to the radiating gas on the external optical axis, an external comparison lamp or a reflector provides radiation through the gas to the instrument.

Sequence of Operation

The position of the rotating choppers of figure 1(b) with respect to the optical axis determines four fluxes A, B, C, and D of radiation seen by the detector. For flux A at chopper 1, internal reference lamp radiation not absorbed by the black surface A is intercepted by chopper 2 to give complete darkness. For flux C at chopper 1, internal reference lamp radiation is reflected from mirror surface C of chopper 1 to the detector. For fluxes B and D, external source radiation is transmitted to the detector. External comparison lamp radiation is present only for D as determined by chopper 3. If, instead of a comparison lamp in figure 1(a), a reflector as shown is used, a doubled path length of gas radiation is present but only for D.

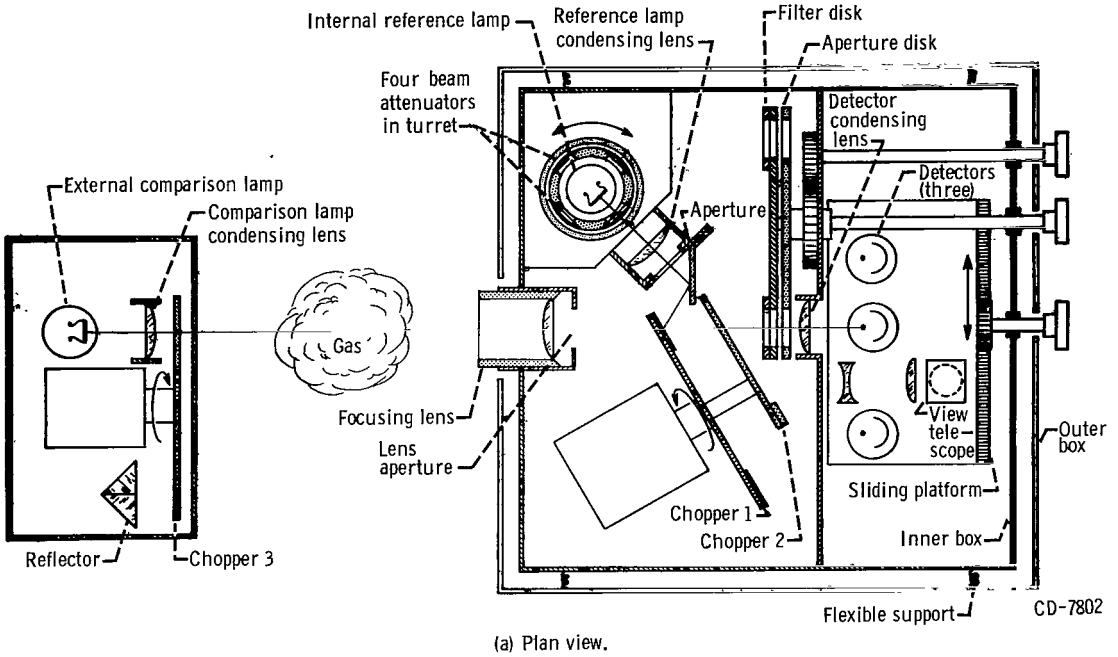

(a) Plan view.

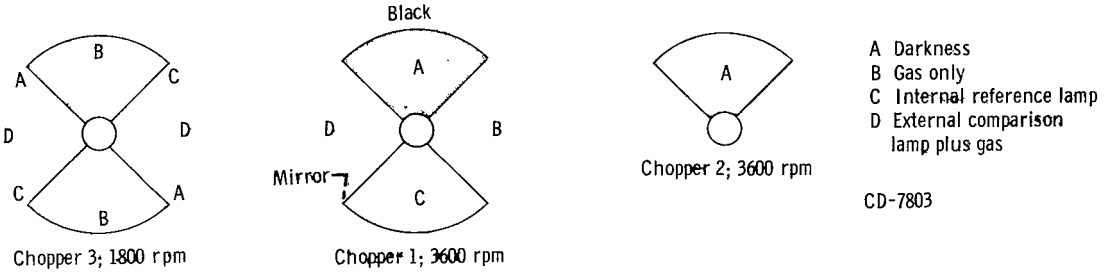

(b) Radiation choppers.

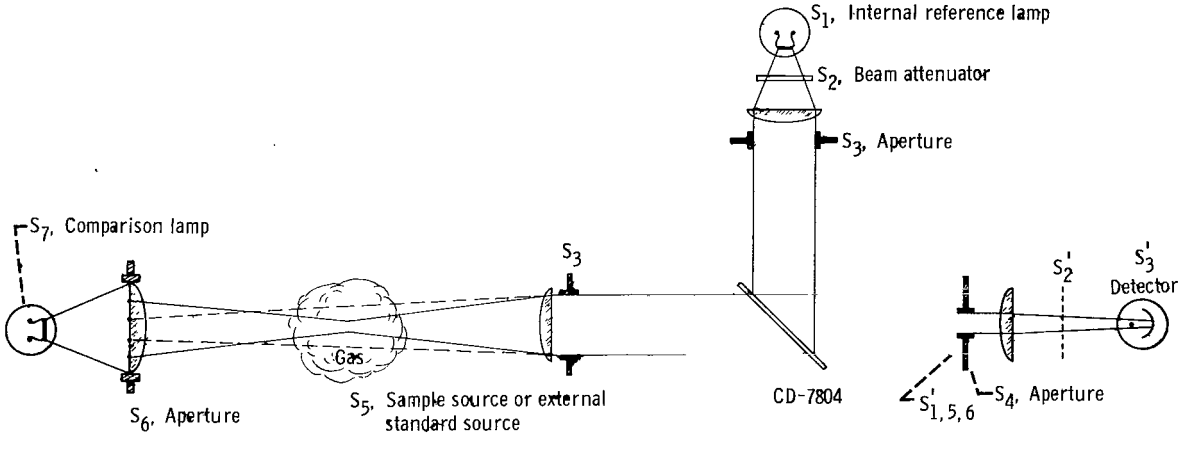

(c) Image and aperture planes.

Figure 1. - Optical system.

Image and Aperture Planes

As discussed in the INTRODUCTION, detector sensitivity varies by much more than 1 percent over the surface of the detector. Thus, for accurate ratios, the same detector area must be uniformly irradiated at each chopper position B, C, and D (fig. 1(b)). In figure 1(c) the image S_3' at the detector is the same size for all sources, since it is the image of identical stops S_3 in the optical path of the sources S_1 and S_5. The image is uniformly irradiated S_3' by an image at $S_{1,5,6}'$ of the sources S_1, S_5, and S_6.

So that the sample radiation can be approximately matched with the internal reference lamp, the lamp intensity is continuously adjustable over a range of 100 by current control, and a beam attenuator at S_2 (fig. 1(c)) may be selected in four steps covering a range of 10^6. Because S_2 is not conjugate to $S_{1,5,6}'$, a simple aperture would not provide uniform irradiance at S_3'. Therefore, S_2 is constructed of a quartz plate in the form of a front-surface mirror; the uncoated surface is fine ground, while the mirror coating is cut into random pinholes by pressing a piece of emery cloth on it. Radiation transmitted by the holes is diffused by the ground surface.

Four or more aperture diameters S_4 are provided by the aperture disk to limit the flux at the photocell or to limit the field of view. Diameters from 0.5 to 0.015 inch provide a flux range of 1000 and a field-of-view range from 6° to 0.2°. The flux-limiting apertures S_4 and S_3 have no refractive elements between them; their geometry is independent of wavelength. The ideal of a fixed geometry is not attained, however, because the sources and the detectors have different shapes, and the lenses have spherical and chromatic aberration. Because the image S_3' is focused by a lens, its focal plane varies with wavelength. Consequently, the transmission factors of apertures S_4 and attenuators S_2 are not independent of the detector, the filter, or each other. The calibration required for every combination is described in the section THEORY.

Depending upon the experiment, either the source at S_5 or the condensing lens at S_6 may be focused at $S_{1,5,6}'$. Inspection of figure 1(c) shows that a focus at S_5 gives a smaller field diameter but requires a larger diameter condensing lens if a comparison lamp is used. A larger condensing lens will have a longer focal length and less magnification of the comparison lamp S_7. The comparison lamp S_7 may be focused at S_5 or S_3. In all cases, the image size must be sufficient to irradiate completely S_5 or S_3, respectively.

For calibration with the external standard lamp, an auxiliary lens had to be added to the focusing lens. This magnified the lamp filament enough to cover the field stop S_2. The transmission factor of the auxiliary lens was measured and multiplied by the lamp radiance.

To focus the radiometer for ultraviolet or infrared wavelengths, one of two methods is used. The new object distance for visual focus may be computed and used, or a supplementary lens may be used during visual focus to compensate for the change of focusing lens power with wavelength.

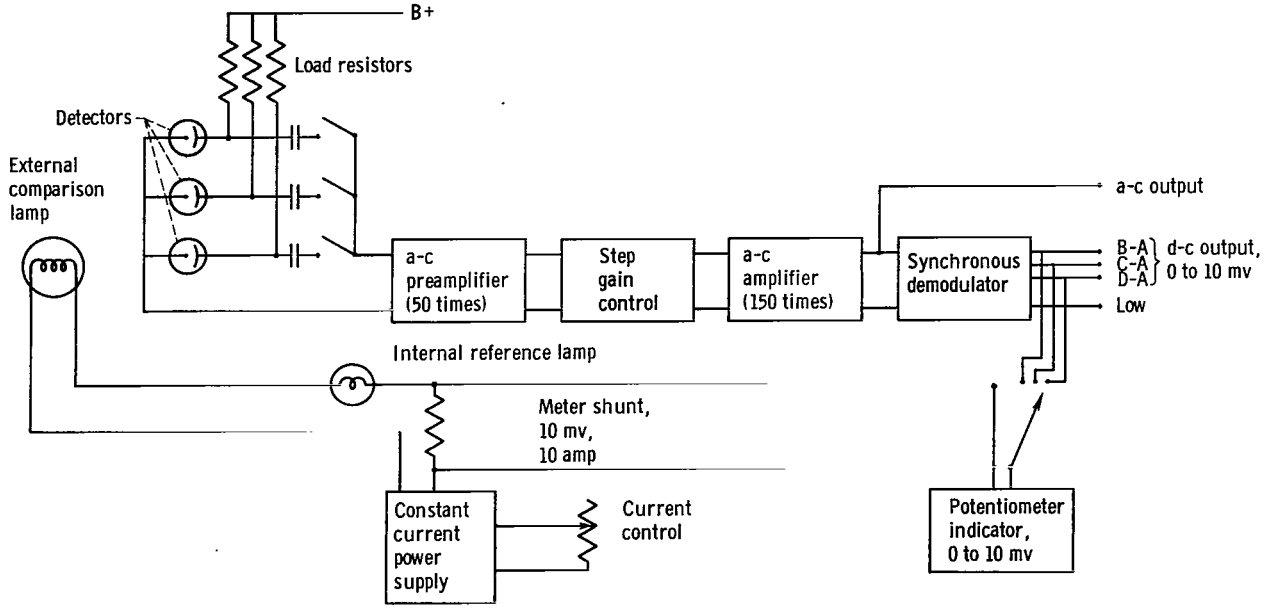

Figure 2. - Electrical block diagram.

Electrical Circuits

In the block diagram of figure 2, the load resistors for each detector are chosen so that the detector-plus-preamplifier noise is twice the preamplifier noise as observed at the recorder output when a resistor is substituted for the detector. Detector noise thus determines the minimum signal detected.

The maximum signal at the preamplifier output is 2×10^5 times the noise. This enables a gain control range of 10^3 with a noise 1 percent of full scale at full gain. The detectors are capable of this dynamic range without overload. A further dynamic range of 10^2 with the multiplier phototube is obtained by reducing the dynode voltage.

The built-in potentiometer indicator is used to set the current of the internal reference lamp for calibration and to read detector output if external recording is not used.

The internal chopper motor is a 3600-rpm synchronous motor with a built-in polarizing magnet. The external chopper motor is 1800-rpm synchronous type. The synchronous demodulator circuit shown in figure 3(a) uses two 60 cps synchronous switches to sort out the fluxes B, C, and D from the detector output waveform shown in figure 3(b). The coupling condenser is grounded by the switch at intervals when zero flux A is present, as shown by the timing curves of figures 3(b). When the fluxes are present, the voltage outputs are the differences V_B-V_A, V_C-V_A, and V_D-V_A. The outputs are filtered with resistance-capacitance networks having time constants of 1 second for high damping, or 0.05 second for low damping.

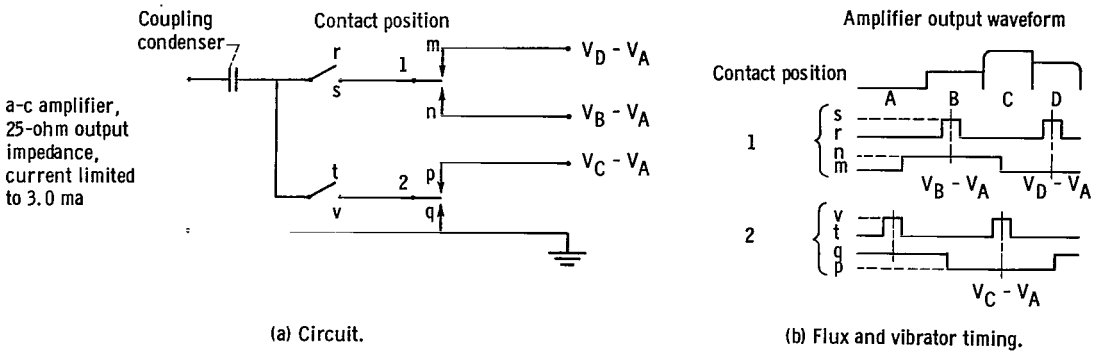

(a) Circuit.

(b) Flux and vibrator timing.

Figure 3. - Synchronous demodulator scheme.

Although the use of a 60-cps line frequency for the chopper motor and the synchronous demodulator with alternating-current coupled amplifiers gives a simple design, there are certain precautions to note. The coupling condenser is common to all three output signals. The current drawn by each output resistor changes the voltage across the coupling condenser during each cycle and introduces some error in the differences V_C-V_A and V_D-V_A. This error is minimized by use of large values of the coupling condenser and the load resistor. The error could be eliminated with an independent demodulation circuit for each output, with a corresponding greater complexity, or with a direct-current buffer amplifier between the coupling condenser and the switch circuit.

The detector output waveform is maintained through the alternating-current amplifiers with a frequency bandwidth from 0.6 to 600 cps. In addition, the flat tops of the 30- and 60-cps square-wave test signals are optimized by a low-frequency-amplitude compensation adjustment.

THEORY

Calibration of Internal Reference Lamp

The detector output voltages V_s, with an external standard source, and $V_{r,s}$, with the internal reference lamp during calibration, are

$$V_s = K \int N_s \epsilon_s \tau R \, d\lambda \tag{1}$$

and

$$V_{r,s} = Kk \int N_r \epsilon_r \tau R \, d\lambda \tag{2}$$

(Symbols are defined in the appendix.) The ratio of equations (1) and (2) yields the calibrated quantity

$$\int N_r \epsilon_r \tau R \, d\lambda = \frac{V_{r,s}}{V_s} \frac{K}{Kk} \int N_s \epsilon_s \tau R \, d\lambda \qquad (3)$$

The quantities on the right side of equation (3) were measured under the following conditions:

(1) The factor K was measured as a voltage with an external source of uniform radiance. Typical data for this instrument are given in the following table:

Nominal aperture diameter, in.	Nominal aperture area factor, K	3100 A (0.31 μ), multiplier phototube	1.9 μ lead sulfide
		Relative output voltage, V	
0.5	1000	640	730
.15	100	92	86
.05	10	9.5	9.3
.015	1	1.00	1.00

(2) The factor Kk was measured as a voltage for all combinations of K and k with internal reference lamp radiation. Typical data for this instrument are given in the following table. Cancellation of K in equation (3) is not possible because, in this table, K and k are not independent of each other. Furthermore, K in the previous table does not agree with K in this table.

Nominal aperture diameter, in.	Nominal aperture area factor, K	Nominal transmission factor, k							
		10^0		10^2		10^4		10^6	
		UV[a]	IR[b]	UV[a]	IR[b]	UV[a]	IR[b]	UV[a]	IR[b]
		Relative output voltage, V							
0.5	1000	5100	----	-----	-----	2.52	2.82	0.0068	0.168
.15	100	740	----	9.1	9.3	.36	.41	.00119	.0266
.05	10	79	71	1.00	1.00	.039	.053	-------	------
.015	1	8.1	6.8	.098	.093	.0052	.0050	-------	------

[a]Ultraviolet at 3100 A (0.31 μ), multiplier phototube.

[b]Infrared at 1.9 μ, lead sulfide.

(3) The integral was numerically integrated by means of standard source calibration data for $N_s \epsilon_s$, relative values of detector response R from manufacturer's data, and relative values of filter transmission factor τ from spectral measurements. Figure 4 shows data used for these calculations with OH and H_2O measurements. The following table lists the calibration constants, the evaluated integral, and the value of equation (2):

Constants of radiometer	3100 A (0.31 μ), multiplier phototube	1.9 μ, lead sulfide
$\int N_s \epsilon_s \tau R \, d\lambda$, w/(ster)(cm^2)	8.75×10^{-4}	0.575
Nominal aperture diameter, in.	0.05	0.015
Aperture area factor, K (table I(a))	9.5	1.00
Nominal attenuator factor	10^o	10^o
Kk (table I(b))	79	6.8
Detector relative output voltage with external standard source, V_s	6170	2050
Detector relative output voltage with internal reference lamp, $V_{r,s}$	1070	1070
$\int N_r \epsilon_r \tau R \, d\lambda$, w/(ster)(cm^2)	1.82×10^{-5}	4.4×10^{-2}

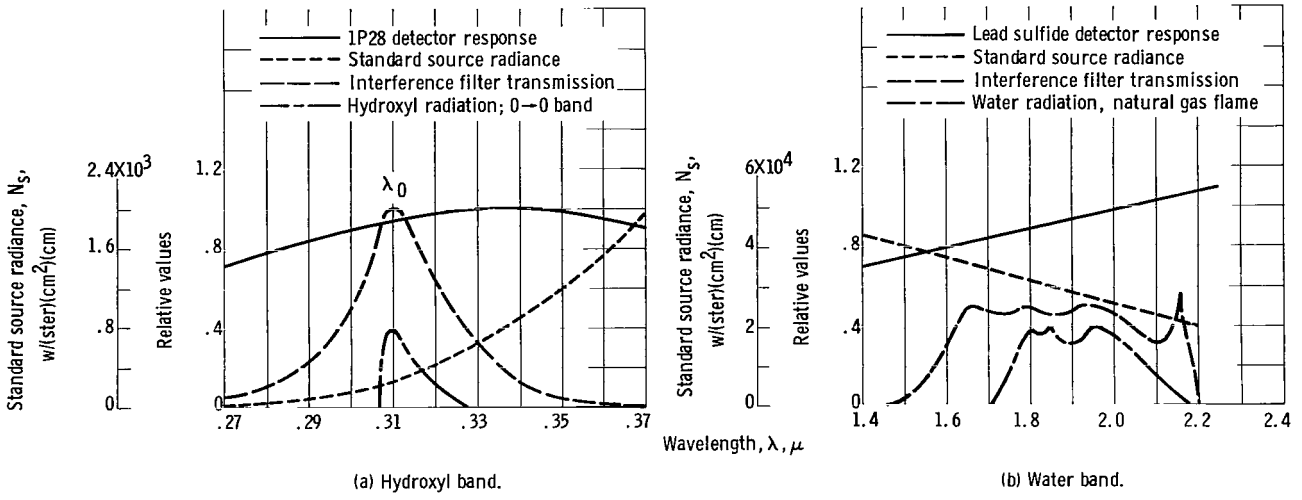

(a) Hydroxyl band.

(b) Water band.

Figure 4. - Spectral distribution.

Absolute Radiation Measurement

The detector output voltages V_x, with sample radiation, and $V_{r,x}$, with the internal reference lamp during the run, are

$$V_x = K \int N_x \epsilon_x \tau R \, d\lambda \tag{4}$$

and

$$V_{r,x} = Kk \int N_r \epsilon_r \tau R \, d\lambda \tag{5}$$

The ratio of equations (4) and (5) yields the measured quantity

$$\int N_x \epsilon_x \tau R \, d\lambda = \frac{V_x}{V_{r,x}} \frac{Kk}{K} \int N_r \epsilon_r \tau R \, d\lambda \tag{6}$$

The voltages corresponding to the proper values of K and Kk and the integral on the right side are given by the previous tables.

For application of equation (6) to the tests in this report, a simplifying assumption is necessary. The OH and H_2O radiation curves of figure 4, which are proportional to the gas emissivity ϵ, have a narrower bandwidth than the curves of N, τ, and R. Thus, N, τ, and R may be treated as constant so that equation (6) is approximated by

$$\int \epsilon_x \, d\lambda = \frac{V_x}{V_{r,x}} \frac{Kk}{K} \frac{\int N_r \epsilon_r \tau R \, d\lambda}{(N_x \tau R)_o} \tag{7}$$

where the subscript o refers to values at the center wavelength of the emission band. The value of $N_{x,o}$ is calculated from the gas temperature as measured. The value of $(\tau R)_o$ is obtained from the table under item (3) in the previous section. The value of $\int \epsilon_x \, d\lambda$ can then be found.

Partial Pressure

With the material in reference 22, the integrated absorption over an absorption band, for a small optical depth where self-absorption is not significant, is

$$\int \alpha_\lambda \, d\lambda = \lambda_o^2 S_{\zeta u} L \frac{273p}{T} \tag{8}$$

where the factor $273p/T$ accounts for the change in $S_{\zeta u}$ from its value at standard temperature and pressure. This equation can be solved for the partial pressure p of the absorbing gas when $S_{\zeta u}$ is given by handbook data (ref. 22) and the other quantities are measured. If Kirchoff's law $\alpha_\lambda = \epsilon_\lambda$ for a gas in thermal equilibrium is used, equations (7) and (8) may be combined to eliminate the common integral and solved for the partial pressure

$$p = \frac{T}{273} \frac{1}{\lambda_o^2 L S_{\zeta u}} \frac{\int N_r \epsilon_r \tau R \, d\lambda}{(N_x \tau R)_o} \frac{V_x}{V_{r,x}} \frac{Kk}{K} \tag{9}$$

where the integral is given in the table under item (3) in the previous section.

Absorption-Emission Method

Partial pressure can be calculated with equation (9) by using gas radiation measurements. The gas spectral emissivity can be near zero. When the emissivity is greater than about 5 percent, it can also be measured with suffi-

cient accuracy by the absorption-emission method, and the partial pressure can then be calculated with equation (8). For this method, a comparison lamp as shown in figure 1 (p. 4) radiates through the gas. Four conditions of flux measurement and the corresponding detector output voltages that may be utilized are

(1) External comparison lamp only:

$$V_1 = K_1 \frac{N_c}{\mathscr{A}} \int_0^{\mathscr{A}} \epsilon_c \int_{\lambda_1}^{\lambda_2} \tau R \, d\lambda \, d\mathscr{A} \tag{10}$$

(2) Gas only with lamp intercepted by chopper:

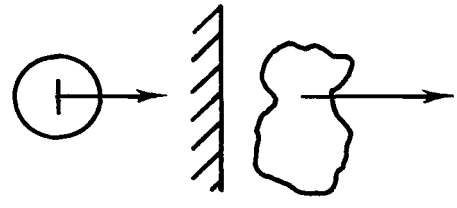

$$V_2 = K_2 N_g \int_{\lambda_1}^{\lambda_2} \epsilon_g \tau R \, d\lambda \tag{11}$$

(3) Gas only with lamp off:

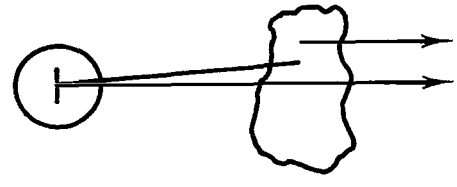

$$V_3 = V_2 + K_3 \tau_3 N_g \int_{\lambda_1}^{\lambda_2} \left[\epsilon_g(1 - \epsilon_g)\right] \tau R \, d\lambda \tag{12}$$

where τ_3 is reflectivity and transmissivity of all elements between gas, lamp, and gas.

(4) Gas and lamp:

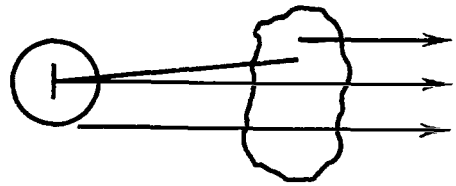

$$V_4 = V_3 + K_4 \frac{N_c}{\mathscr{A}} \int_0^{\mathscr{A}} \epsilon_c \int_{\lambda_1}^{\lambda_2} (1 - \epsilon_g)\tau R \, d\lambda \, d\mathscr{A} \tag{13}$$

The radiances $N_c\epsilon_c$ and N_g may be placed outside the wavelength integral because they are essentially constant over the bandwidth made narrow by choice of the filter τ or by the selected band of gas emissivity ϵ_g.

For absolute measurements using the internal reference lamp, voltages V_1 to V_4 may be corrected by writing equation (6) in the form of equations (10) to (13) as

$$V_x\left(\frac{Kk}{V_{r,x}} \int N_r \epsilon_r \tau R \, d\lambda\right) = K \int N_x \epsilon_x \tau R \, d\lambda \tag{14}$$

where the quantity in parenthesis is the correction factor to V_x and thus to V_1 to V_4.

Of the four conditions of flux measurement, voltages V_2 and V_3 are both from gas radiation, but they have an important difference not generally recognized. Voltage V_2 is obtained with a rotating chopper that intercepts lamp radiation, while V_3 is obtained by turning the lamp off. Voltage V_3 contains an extra component, gas radiation reflected from the lamp, the windows, and other elements between the lamp and the gas. Thus V_3 is present with line-reversal measurements, but V_2 is present with absorption-emission measurements using a light chopper.

In the equations for V_1 and V_4, the differential area $d\mathscr{A}$ represents a lamp with emittance that varies over its area $\mathscr{A}$ or a lamp that only partially fills the area of the detector. It will be seen that the variable area vanishes for gas emissivity measurements but not for temperature measurements.

Gas Emissivity by Absorption Emission

For an experiment in which the bandwidth of equations (10) to (13) is limited by either ϵ_g or τ but the bandwidth of ϵ_g is less than τ (see fig. 4), equation (10) substituted in equation (13) yields

$$V_4 = V_3 + \frac{K_4}{K_1} V_1 \left(1 - \frac{\int_{\lambda_1}^{\lambda_2} \epsilon_g \, d\lambda}{\int_{\lambda_1}^{\lambda_2} \tau \, d\lambda} \right) \tag{15}$$

The integrated gas emissivity is

$$\int_{\lambda_1}^{\lambda_2} \epsilon_g \, d\lambda = \frac{\frac{K_4}{K_1} V_1 + V_3 - V_4}{\frac{K_4}{K_1} V_1} \left(\frac{\int_{\lambda_1}^{\lambda_2} \tau \, d\lambda}{\tau_o} \right) \tag{16}$$

When it is desirable to leave the lamp on and to use a chopper, a voltage ratio G may be determined initially and used throughout the experiment, where

$$G = \frac{V_3}{V_2} \tag{17}$$

Then equation (16) becomes

$$\int_{\lambda_1}^{\lambda_2} \epsilon_g \, d\lambda = \frac{\frac{K_4}{K_1} V_1 + GV_2 - V_4}{\frac{K_4}{K_1} V_1} \left(\frac{\int_{\lambda_1}^{\lambda_2} \tau \, d\lambda}{\tau_o} \right) \tag{18}$$

Equation (16) or (18) is used to calculate partial pressure with equation (8).

For a bandwidth limited by the filter τ (eqs. (10) to (13)) instead of by gas emissivity ϵ_g, equations (16) and (18) are also obtained, ϵ_g is a constant $\epsilon_{g,o}$ over the bandwidth, and the term containing τ cancels out.

Gas Temperature by Absorption Emission

Temperature is obtained from the ratio N_g/N_c, as given by Wien's thermal radiation equations, $N_g = c_1 \lambda^{-5} \exp(-c_2/\lambda T_g)$ for the gas thermal temperature T_g and $N_c \epsilon_c = c_1 \lambda^{-5} \exp(-c_2/\lambda T_c^*)$ for the comparison lamp radiance temperature T_c^*. The result is

$$T_g = \frac{T_c^*}{1 + \frac{\lambda T_c^*}{c_2} \ln \frac{N_c \epsilon_c}{N_g}} \tag{19}$$

Substitution of $N_c\epsilon_c/N_g$, obtained from equations (10), (11), and (18), yields

$$T_g = \frac{T_c^*}{1 + \frac{\lambda T_c^*}{c_2} \ln \frac{\frac{K_4 V_1}{K_1} + GV_2 - V_4}{\frac{K_4 V_2}{K_2}} \gamma} \tag{20}$$

where

$$\gamma = \frac{\epsilon_c}{\frac{1}{\mathscr{A}} \int_0^{\mathscr{A}} \epsilon_c \, d\mathscr{A}} \tag{21}$$

The factor γ is generally made unity by use of a uniform-radiance source that fills the field of view of the instrument.

For line-reversal temperatures where $V_1 = V_4$, the voltage ratio G (eq. (17)) appears as a correction to the comparison lamp radiance temperature, with a gas temperature of

$$T_g = \frac{T_c^*}{1 + \frac{\lambda T_c^*}{c_2} \ln G} \tag{22}$$

where $K_4 = K_1 = K_2$.

TESTS

The tests demonstrate the use of the instrument as a radiometer-pyrometer by comparing partial pressures in the products of combustion as measured and as calculated from theory. Measurements were made of OH radiation at 3100 A, H_2O radiation at the 1.9-micron band in the infrared spectrum, and gas temperature by absorption-emission of the sodium D lines. These data were used to calculate the partial pressure of OH and H_2O. The theoretical partial pressure of the equilibrium products of combustion were computed by the method of reference 23, given the fuel and oxidant composition, the equivalence ratio, the pressure, and the temperature. This was done on a computer programmed for such work at Lewis.

The first test was made with a Meker burner modified by a rectangular extension tube to produce a two-dimensional flame with a 1.1-centimeter depth along the optical path. When natural gas and air were burned, the average absorptivity for the 1.9-micron H_2O band was less than 0.01, which was too small for temperature measurement. Instead, sodium bicarbonate was introduced

and temperature was measured at the sodium D lines by absorption-emission with a filter of 15-A bandwidth. Temperature was measured also by sodium line reversal with a spectroscope and the same comparison lamp. Both methods agreed to within ±10° K. The results of OH and H_2O measurements are as follows:

Test results	Natural gas and air		Gasoline and air	
	Theoretical	Experimental	Theoretical	Experimental
	Partial pressure of emitter, atm			
OH at 0.31 μ	0.00148	0.00118	0.00036	0.000238
H_2O at 1.90 μ	.183	.309	.110	.139
$(OH)_{exp}/(OH)_{th}$	0.80		0.66	
$(H_2O)_{exp}/(H_2O)_{th}$	1.70		1.31	
$(OH/H_2O)_{exp}/(OH/H_2O)_{th}$	0.47		0.50	

The test conditions were the following:

Test data	Natural gas and air		Gasoline and air	
Sodium-line-reversal temperature, °K	2095		1856	
Absorption-emission temperature, °K	2088		1861	
Static pressure, atm	1.0		0.86	
Flame depth, cm	1.1		7.0	
Fuel-air-ratio determination	Maximum radiation of H_2O		Measured equivalence ratio of 0.9772	
	OH at 2095° K	H_2O at 2095° K	OH at 1900° K	H_2O at 1835° K
Integrated absorption coefficient, $S_{\lambda u}$, $(cm^{-2})(atm^{-1})$ at standard temperature and pressure	3.07×10^5	30	-----	--------
Center-wavelength radiance N_o at reversal temperature	9.1	1.37×10^5	1.024	7.89×10^4
Detector relative output voltage with sample radiation, V_x	63	50	146	148
Detector relative output voltage with internal reference lamp during run, $V_{r,x}$	687	81.8	286	136
Nominal aperture diameter, in.	0.05	0.05	0.15	0.15
Aperture area factor, k	9.5	9.3	92	86
Attenuator setting	10^2	10^2	10^4	10^2
Attenuation factor, Kk	1.00	1.00	0.36	9.3
Center-wavelength transmission factor, τ_o	0.62	0.47	0.57	0.43
Center-wavelength detector relative response, R_o	.94	.94	.94	.94

Tests were also made with a high-velocity jet (Mach 0.5) of the combustion products of gasoline and air (ref. 24). (The results and the test conditions are also shown in the preceding tables.) The gas radiation showed intensity fluctuations. Because of the highly nonlinear relation between radiance and temperature, these fluctuations caused the average gas radiance to be greater

than the radiance corresponding to the average gas temperature. Consequently, the optically determined average temperature was also greater than the average gas temperature (ref. 25). The error was 27° K for the sodium-line-reversal temperature. The error depends on wavelength, since it is 71° K for OH and 6° K for H_2O. Therefore, temperatures of 1900° K for OH and 1835° K for H_2O were used in the calculation of measured partial pressure. In the calculation of theoretical partial pressure, a temperature of 1849° K for OH and 1856° K for H_2O was applied to account for the nonlinear relation between partial pressure and temperature in accordance with reference 25.

SUMMARY OF PERFORMANCE FEATURES

The following tabulation summarizes the performance and limitations of the instrument:

Spectral range	That of fused-quartz optics	
Frequency response		
Demodulated output, cps	0.16 or 3	
Modulated output, cps	30	
Unmodulated output, cps	600	
Field of view, radians	0.003 to 0.1	
Diameter of focusing-lens aperture, in.	1/2	
Dynamic range of flux measurement		
External standard source		
Aperture	10^6	
NBS lamp intensity	[a]$\sim 10^2$	
Total	$\sim 10^8$	
Sample and external standard source	Multiplier phototube	Photoconductor
Aperture	10^3	10^3
Amplifier gain	10^3	10^3
Detector gain	10^2	---
Total	10^8	10^6
Noise equivalent input power[b]	To instrument	To detector[c]
1P28 multiplier phototube, 3100 A, w	4×10^{-15}	1×10^{-15}
4- by 4-mm lead sulfide cell, 1.9 μ, w	30×10^{-11}	2×10^{-11}
4- by 4-mm lead selenide cell, 1.9 μ, w	80×10^{-9}	2×10^{-9}

[a]Depends on wavelength.

[b]With 1-sec time constant and interference filter.

[c]Manufacturer's specification.

Lewis Research Center
National Aeronautics and Space Administration
Cleveland, Ohio, February 2, 1964

APPENDIX - SYMBOLS

A	zero flux condition
$\mathscr{A}$	area of source, cm^2
B	flux from external source
C	flux from internal reference lamp
c_1	Planck's radiation constant, 1.19×10^{-5} (erg)(cm^2)/sec
c_2	Planck's radiation constant, 1.438 (cm)(^oK)
D	flux from external source plus flux from external comparison lamp
G	voltage ratio
K	geometrical factor of optical system
k	transmission factor of attenuator for internal reference lamp
L	path length through gas, cm
N	radiance, w/(ster)(cm^2)(cm)
p	partial pressure, atm
R	detector response, v/w
S	aperture stop
S'	image of aperture stop
S_{lu}	integrated absorption coefficient, (cm^{-2})(atm^{-1}) at standard temperature and pressure
T	temperature, ^oK
T^*	radiance temperature, ^oK
V	voltage, v
α	absorptivity
γ	correction factor for nonuniform emissivity
ϵ	emissivity
λ	wavelength, cm or μ

τ	transmission factor

Subscripts:

A,B,C,D	fluxes A,B,C,D
c	comparison lamp
exp	experimental
g	gas
o	center wavelength of band
r	internal reference lamp
s	value during calibration, or standard lamp
th	theoretical
x	value during test
λ	wavelength

REFERENCES

1. Schmidt, H.: Prüfung der Strahlungsgesetze der Bunsen-Flamme (Proof of the Radiation law in the case of the Bunsen Flame). Ann. d Physik, vol. 29, 1909, pp. 971-1028.

2. Jacobs, Donald H. and Scholnick, S.: The Absorption - Emission Pyrometer: A New Type of Instrument for the Measurement of High Flame Temperatures. North Amer. Rept. AL-100, (1947).

3. Silverman, S.: Determination of Flame Temperatures by Infra-Red Radiation. J. Opt. Soc. Am., vol. 39, 1949, pp. 275-277.

4. Curcio, J. A., Stewart, H. S., and Petty, C. C.: A Method for Determination of Flame Temperature from Emission in Ultraviolet OH Band. J. Opt. Soc. Am., vol. 41, 1951, pp. 173-179.

5. Heidmann, M. F. and Priem, R. J.: Modified Sodium-Line-Reversal Technique for Measurement of Combustion Temperatures in Rocket Engines, J. Am. Rocket Soc., vol. 23, 1953, pp. 248-253.

6. Kivenson, G.: Some Considerations in Design of Double-Beam Analyzers for Industrial Control. J. Opt. Soc. Am., vol. 40, 1950, pp. 112-118.

7. Williams, Van Zandt, Hawes, R. C. and Gallaway, W. S.: Principles of Infrared Spectrophotometry. Science, vol. 113, 1951, pp. 51-54.

8. Young, Andrew T.: Temperature Effects in Photomultipliers and Astronomical Photometry. Applied Optics, vol. 2, 1963, pp. 51-60.

9. Yang, C. C. and Legallais, V.: Rapid and Sensitive Recording Spectrophotometer for Visible and Ultraviolet Region. I. Description and Performance. Rev. Sci. Instr., vol. 25, 1954, pp. 801-812.

10. Markov, M. N. and Kruglyakov, E. P.: Zonal Sensitivity of PbS Photoconductors. Optics and Spect., vol. 7, 1960, pp. 284-285.

11. Kessler, K. G. and Wolfe, R. A.: Measurement of Intensity Ratios of Spectral Lines with Electron Multiplier Photo-Tubes. J. Opt. Soc. Am., vol. 37, 1947, pp. 133-144.

12. Wormser, E. M.: Properties of Thermistor Infrared Detectors. J. Opt. Soc. Am., vol. 43, 1953, pp. 15-21.

13. Gibson, A. F.: Sensitivity and Response Time of Lead Sulphide Photoconductive Cells. Proc. Phys. Soc., vol. 64B, 1951, pp. 603-615.

14. Potter, R. F., Pernett, J. M., and Naugle, A. B.: Measurement and Interpretation of Photodetector Parameters. Proc. I.R.E., vol. 47, (1959), pp. 1503-1507.

15. Pyatt, E. C.: Brightness Temperature Pyrometer Using Photoconductive Cell. J. Sci. Instr., vol. 29, 1952, pp. 125-127.

16. Harmer, J. D. and Watts, B. N.: Infra-Red Radiation Pyrometer: J. Sci. Instr., vol. 32, 1955, pp. 167-170.

17. Lord, J. S.: Design and Performance Characteristics of an Automatic Brightness Pyrometer. In: Temperature; Its Measurement and Control in Science and Industry. (Herzfeld, C. M. ed.) Vol. 3, pt. 2, Reinhold Publishing Corp., 1962, pp. 865-872.

18. Derganc, W. and Howell, S. N.: Two New Total Radiation Pyrometers. A.I.E.E. Trans., vol. 75, pt. I, 1965, pp. 360-367.

19. Astheimer, R. W. and Wormser, E. M.: High-Speed Infrared Radiometers J. Opt. Soc. Am., vol. 49, 1959, pp. 170-183.

20. Grum, F.: Modification of a Beckman Spectrophotometer for Direct Measurements of Spectral Energy Distribution of Light Sources, Appl. Optics, vol. 2, 1963, pp. 237-242.

21. Stair, R., Johnston, R. G., Halbach, E. W.: Standard of Spectral Radiance for the Region of 0.25 to 2.6 Microns. J. Res. NBS, vol. 64A, no. 4, 1960, pp. 291-296.

22. Penner, S. S.: Quantitative Molecular Spectroscopy and Gas Emissivities, Addison-Wesley Pub. Co., 1959, ch. 2.

23. Zeleznik, Frank J. and Gordon, Sanford: A General IBM 704 or 7090 Computer Program for Computation of Chemical Equilibrium Compositions, Rocket Performance, and Chapman-Jouguet Detonations. NASA TN D-1454, 1962.

24. Glawe, George E. and Shepard, Charles E.: Some Effects of Exposure to Exhaust-Gas Streams on Emittance and Thermoelectric Power of Bare-Wire Platinum Rhodium-Platinum Thermocouples. NACA TN 3253, 1954.

25. Buchele, Donald.: Nonlinear-Averaging Errors In Radiation Pyrometry. NASA TN D-2406, 1964.

2-17-67

"The aeronautical and space activities of the United States shall be conducted so as to contribute . . . to the expansion of human knowledge of phenomena in the atmosphere and space. The Administration shall provide for the widest practicable and appropriate dissemination of information concerning its activities and the results thereof."

—NATIONAL AERONAUTICS AND SPACE ACT OF 1958

NASA SCIENTIFIC AND TECHNICAL PUBLICATIONS

TECHNICAL REPORTS: Scientific and technical information considered important, complete, and a lasting contribution to existing knowledge.

TECHNICAL NOTES: Information less broad in scope but nevertheless of importance as a contribution to existing knowledge.

TECHNICAL MEMORANDUMS: Information receiving limited distribution because of preliminary data, security classification, or other reasons.

CONTRACTOR REPORTS: Technical information generated in connection with a NASA contract or grant and released under NASA auspices.

TECHNICAL TRANSLATIONS: Information published in a foreign language considered to merit NASA distribution in English.

TECHNICAL REPRINTS: Information derived from NASA activities and initially published in the form of journal articles.

SPECIAL PUBLICATIONS: Information derived from or of value to NASA activities but not necessarily reporting the results of individual NASA-programmed scientific efforts. Publications include conference proceedings, monographs, data compilations, handbooks, sourcebooks, and special bibliographies.

Details on the availability of these publications may be obtained from:

SCIENTIFIC AND TECHNICAL INFORMATION DIVISION

NATIONAL AERONAUTICS AND SPACE ADMINISTRATION

Washington, D.C. 20546